Mm and Sub-mm Properties of Ramp-Type Josephson Junctions on MgO with STO Buffer Layers

H. Myoren†, J. Chen, and T. Yamashita
Research Institute of Electrical Communication, Tohoku University, 2-1-1 Katahira, Aoba-ku, Sendai 980-8577, Japan

L. Amatuni, A.H. Sonnenberg, G.J. Gerritsma, and H. Rogalla
Low Temperature Division, Fac. of Applied Physics, University of Twente, P.O.Box 217, 7500 AE Enschede, The Netherlands

***Abstract*—We have successfully fabricated ramp-type junctions on MgO substrates using an $SrTiO_3$ (STO) buffer layer. The observed I_cR_n product for the junctions on MgO with STO buffer layer were about 2mV at 4.2K and 0.1mV at 60K. The junctions clearly showed Shapiro steps under irradiation of mm-waves and sub-mm-waves. We observed Josephson emission at 50GHz from a junction on a MgO substrate with STO buffer layer at 17K. We have also confirmed mixing in the self-oscillating mode using mm-wave and sub-mm-wave signals.**

I. Introduction

Fabrication technology of high-T_c ramp-type Josephson junctions (JJs) is one of the promising technologies for superconducting electronics, because of its reproducibility and flexibility of junction parameters. These junctions seem to be suitable for not only digital circuits but also high-frequency applications. High-T_c ramp-type JJs with $PrBa_2Cu_{3-x}Ga_xO_{7-\delta}$ (PBCGO) barriers fabricated on $SrTiO_3$ (STO) substrates have been reported to have relatively high-I_cR_n (I_c is the critical current and R_n is the normal resistance of the junction) products of 8mV at 4.2K[1] and this property is implying THz response and high-temperature operations.

To realize high-frequency operation, we need to develop a fabrication technique of ramp-type JJs on suitable substrates for high-frequency operation, such as MgO and Al_2O_3. We have already succeeded in fabricating ramp-type JJs with PBCGO barrier layers on MgO and showed THz response[2]. However, I_cR_n products of the JJs were still small[2].

In this study, we demonstrate improved junction properties using MgO substrates with STO buffer layers. Moreover, we show observed mm and sub-mm wave response of the JJs.

Manuscript received September 15, 1998.

†present address: Dept. of Electrical and Electronic Systems, Fac. of Engineering, Saitama University, 255 Shimo-Okubo, Urawa, Saitama 338-8570, Japan. Tel:+81-48-858-3763, Fax:+81-48-858-3473, e-mail:myoren@super.ees.saitama-u.ac.jp

This work was supported in part by the Core Research for Evolutional Science and Technology (CREST) of Japan Science and Technology Corporation (JST) and by the EC Esprit programme under contact number 23429.

II. Experimental

High-T_c ramp-type JJs were fabricated on MgO(100) substrates. In this study, we used $DyBa_2Cu_3O_{7-\delta}$ (DBCO) as base and top high-T_c superconducting electrodes and PBCGO as isolation between the electrodes and barrier layers for JJs. In the case of PBCGO barrier layers deposited directly on MgO, the high deposition temperature resulted in a very rough surface morphology for highly Ga-doped PBCGO. Thus, we used STO buffer layers to avoid direct deposition of the PBCGO barrier layers on MgO after ramp structuring. Optimized deposition conditions are listed in Table I. Using STO buffer layers, we could use the same deposition conditions as those for ramp-type JJs on STO substrates.

The fabrication process of our JJs was similar to that on STO substrate described previously[3], except for deposition and etching of STO buffer layers. Starting from a sputtered STO/DBCO/PBCGO(x=0, 0.1) triple layer, a ramp with an angle of ~20° with respect to the substrate surface was etched using an Ar-ion beam. We carefully stopped etching at the middle of STO buffer layer and left a thin STO layer to grow a high-quality PBCGO barrier and DBCO counterelectrode on the etched surface. The ramp surface was subsequently ion-beam cleaned at low energy to remove damage from the interface. Next, the ramp was covered by a PBCGO(x=0 and 0.1) barrier layer and a DBCO counterelectrode. Final junction definition, wiring, and metallization were performed by a conventional photolithographic process. The barrier thickness d for JJs was inferred from the calibrated growth rate.

After film deposition, we confirmed in-plane-orientation of the films using an X-ray diffraction (XRD) method (ϕ-scan) and observed surface morphology by an atomic force microscopy (AFM).

TABLE I
Sputtering Conditions for STO, DBCO and PBCGO Films.

Target	STO	DBCO	PBCGO
Sputtering gas[a]	Ar+O_2	Ar+O_2	Ar+O_2
Gas flow ratio	15:20	15:20	15:20
Gas pressure (Pa)	25	35	23
Sub. temp. (°C)	770	770	790
Rf power (W)	90	90	90
Dep. rate (nm/min)	0.67	0.93	1.8
Thickness (nm)	40	120	150

[a]a trace of H_2O vapor gas was added.

TABLE II
WAVELENGTH, FREQUENCY AND OUTPUT POWERS OF FIR SIGNALS FOR DIFFERENT GASES.

Molecule gases	Wavelength (μm)	Frequency (THz)	Output Power (mW)
CH_2OH	118.8	2.524	120
CH_2F_2	184.3	1.627	150
HCOOH	393.6	0.762	40

I-V curves were measured with a conventional four-probe method. For high-frequency measurements, the topology of electrodes of JJs was a bow-tie antenna structure. Millimeter waves (100GHz) were generated by a Gunn diode, and were fed to the ramp-type JJs using a waveguide. Sub-millimeter wave signals were generated by a far-infrared (FIR) laser, pumped by a 38W CO_2 laser. Wavelength, frequency and output power of the signals are listed in Table II for three different gases. THz wave signals were fed to the JJs mounted on a cold stage in an infrared cryostat via a quasi-optical system consisting of a TPX lens and a hyperhemispherical lens made of high resistivity Si.

III. RESULTS

A. Quality of STO Buffer Layers on MgO

STO buffer layers were deposited on MgO(100) substrates by off-axis rf-magnetron sputtering. Deposition conditions for STO buffer layers were optimized with respect to surface smoothness. Though we tried to use annealed MgO substrates with surfaces covered with terraces and unit-cell-height steps[4], this resulted in a relatively rough surface of the STO layer. So, we used as-received MgO substrates in this study.

Figure 1 shows an AFM image of 1×1 μm^2 for the 40nm-thick STO buffer layer on a MgO substrate deposited using optimized conditions. The surface was covered with terraces of half or one unit-cell-height steps. The surface roughness of the buffer layers is smaller than 0.2 nm rms, comparable to that of as-received MgO(100) substrates.

In-plane-orientation of buffer layers is also very important to get high-quality ramp-type JJs. If the STO buffer layers contain rotated grains, tilted grain boundaries are generated and undesirable grain boundary junctions might be caused in the electrodes.

Figure 2 shows an XRD ϕ-scan for an STO buffer layer with respect to the (110) reflection of STO. The reflection peaks are only observed for the rotation angles of 45°, 135°, 225° and 315° at which the (440) reflection peaks of MgO substrate are also observed.

These results showed that STO(100) buffer layers were grown epitaxially on MgO(100) with the relation of STO<001>//MgO<001>. This means that we could treat MgO(100) substrates with STO buffer layer as

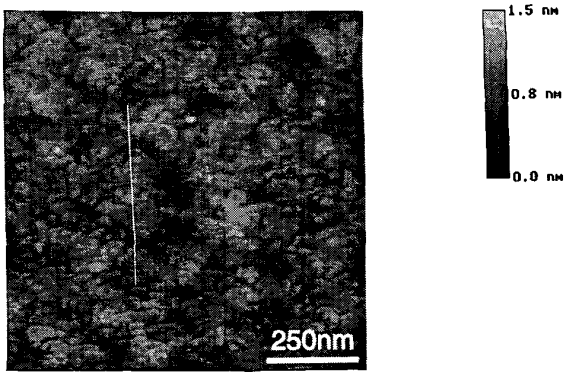

Fig. 1. AFM 1×1μm^2 image of a 40nm-thick STO buffer layer on a MgO(100) substrate. The rms roughness is 0.13nm along the line.

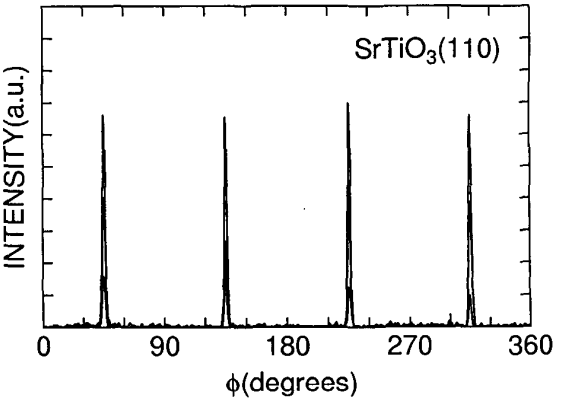

Fig. 2. ϕ-scan of (110)-planes for STO buffer layer on a MgO(100) substrate.

STO(100) substrates. As a result, we consistently obtained 100nm-thick DBCO films with T_c of 89K and 300nm-thick DBCO films with T_c of 91K and J_c(77K) of $5\times10^6 A/cm^2$.

We also confirmed epitaxial growth of PBCGO films on MgO substrates with STO buffer layer even at high deposition temperature of 790°C. Surface morphology of the PBCGO films was smooth enough to fabricate multilayer structures.

B. Electrical Properties of the Junctions

Considering mm and sub-mm wave applications, STO buffer layers on MgO were as thin as possible because of its dielectric properties. However we needed a certain thickness of the STO layers from the view point of processing the ramp-structures. We had to leave a thin STO layer to grow the following PBCGO and DBCO layers. So, we deposited 40nm-thick STO buffer layers on the MgO substrates for making the ramp-type JJs since the etching rate of the STO layer using 500eV Ar^+ ions was about 18nm/min and we could manage to stop the etching at the middle of STO layers.

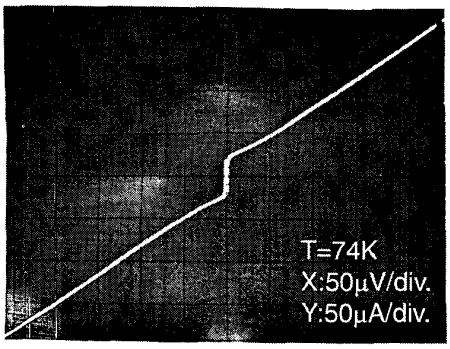

Fig. 3. I-V curve of a ramp-type JJ on MgO(100) with 40nm-thick STO buffer layer at 74K.

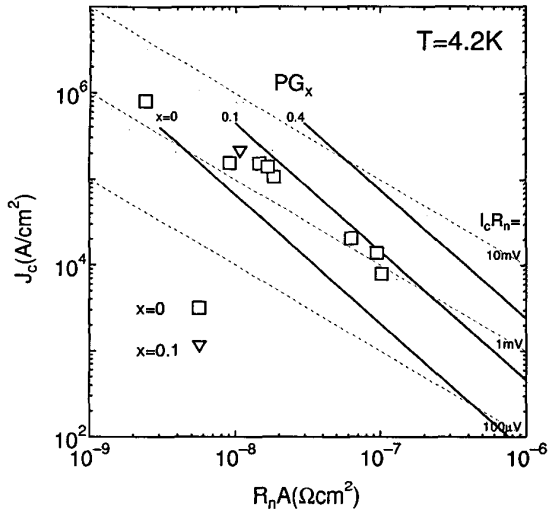

Fig. 4. Relationship between J_c and R_nA for ramp-type JJs on MgO(100) with STO buffer layers at 4.2K.(□:x=0 and ▽:x=0.1) Three solid lines show typical J_c vs. R_nA relations for JJs with three different doping levels (x=0, 0.1 and 0.4) on STO substrates

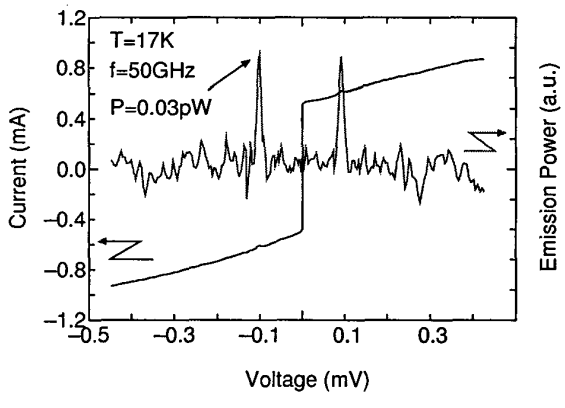

Fig. 5. I-V curve and Josephson emission peaks at 50GHz of a ramp-type JJ on a MgO(100) substrate with 70nm-thick STO buffer layer at 17K. R_n of this JJ is 2Ω.

Figure 3 shows a current-voltage (I-V) curve of a ramp-type JJ with 10nm-thick PBCGO (x=0) barrier at 74K. The observed characteristics can be very well described by the resistively shunted Josephson junction (RSJ) model. The normal resistance of the JJs decreases with increasing temperature and increasing bias voltage. These electric transport properties of the ramp-type JJs with PBCGO barrier are well described by a combination of direct tunneling and resonant tunneling via localized states as already reported for the ramp-type JJs on STO substrates[5].

The I_cR_n product of this junction was 2.4mV at 4.2K and 0.1mV at 60K. I_c could be observed up to 83K. Figure 4 shows the relationship between J_c and R_nA (A is junction area) of the JJs with PBCGO (x=0, 0.1) barriers on STO buffered MgO substrates. Three solid lines in the figure show typical J_c vs. R_nA relations for JJs with three different doping levels (x=0, 0.1 and 0.4) on STO substrates, reported previously[1]. I_cR_n products are almost constant and larger than those for the JJs on STO. This suggests that we would get JJs with large I_cR_n products using more high Ga-doped PBCGO barriers.

C. Mm and Sub-mm Wave Properties of the Junctions

Understanding the origin and limit of the intrinsic noise in high frequency devices is a key point for their applications. At first, we observed Josephson self-emission from a ramp-type JJ fabricated on MgO and estimated the intrinsic noise of the JJ.

The sample was mounted in the waveguide section coupled via impedance transformer to the standard K-band waveguide. The Josephson self-emission was measured at 50GHz by a high sensitivity microwave radiometer, with a bandwidth Δf_{IF}=0.9GHz for the intermediate frequency (IF) amplifier (f_{IF}=1.3GHz), and an integration time constant of 4s. Figure 5 shows the I-V curve of a JJ measured at 17K and corresponding power vs. voltage dependence at 50 GHz. R_n of this JJ was 2Ω. Two Josephson emission peaks are seen around zero voltage. These peaks are symmetrically located and have equal amplitude corresponding to RSJ theoretical model. The peak voltages of ±0.1mV are in good agreement with the frequency of the receiver as given by the Josephson relation $V_J = \Phi_0 f_e$, where Φ_0 is the flux quantum and f_e is the frequency of Josephson emission. Maximum detected power at frequency 50 GHz was of 0.03 pW. The measured emission linewidth Δf_m for the same junction at 50 GHz is 4.0GHz. This experimental value of emission line-width is about 4 times higher than the minimum possible linewidth estimated by RSJ-model equation[6] $\Delta f_T = \frac{4\pi}{\Phi_0^2} k_B T R_D^2 / R_n$=0.94GHz, where k_B is the Boltzman's constant and R_D the dynamic resistance of the JJ. However this value is much better than values measured for HTS step-edge and bi-crystal junctions at similar frequencies[7].

We examined the highest detected frequency of the JJs

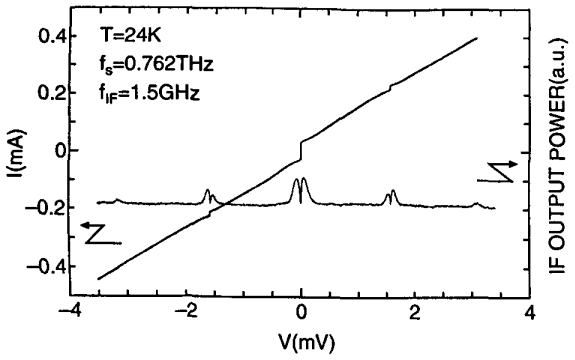

Fig. 6. *I-V* curve under irradiation of 0.762THz signal from a FIR laser and self-mixing IF(1.5GHz) output power curve using Josephson self-emission as a LO source of a ramp-type JJ on MgO(100) with STO buffer layer at 24K

using mm and sub-mm wave signals from a Gunn oscillator and a FIR laser. 100GHz mm wave signals were easily coupled to the JJs and Shapiro steps could be observed up to 10mV at the maximum signal power. Fundamental mixing behavior was also confirmed in the mm-wave range.

In the sub-mm wave region, we obtained Shapiro steps in *I-V* curves under irradiation of 0.762THz signals from the FIR laser. At higher frequencies, listed in Table II, irradiation measurements were not so successful possibly due to the high signal-absorbing properties of the STO buffer layer.

We also tried to observe Josephson self-oscillator mixing behavior of the ramp-type JJs under irradiation from the FIR laser. This mixing mode is very attractive for high frequency applications in high sensitivity heterodyne receivers[6], [8]. In this mixing mode, the Josephson self-oscillation works as a local oscillation and IF signals appear at the frequency of $f_{IF} = |n \cdot f_s - f_J| \leq f_s$, where n is integer. Since f_{IF} is of order of 1~10GHz, IF output power peaks appear at both sides of the voltages of the Shapiro steps. In our experiments, IF signals were amplified using a low-noise amplifier (noise temperature T_N=12K and gain G=30dB) followed by a band-pass filter (f_c=1.5GHz and Δf=0.4GHz) and then detected by a high-sensitive wideband diode detector.

Figure 6 shows *I-V* curve under irradiation of 0.762THz sub-mm wave signal from the FIR laser. Clear Shapiro steps can be seen at ±1.58mV and ±3.16mV. On the screen of the oscilloscope, third Shapiro steps could be observed. Figure 6 also shows IF output power (1.5GHz) from the JJ under irradiation of 0.762THz. Linewidth of IF signals also corresponds to that of Josephson self-oscillation. Δf_m for IF signal of about 150GHz was rather large. However this value is a few times as large as the value estimated using R_n=8.5Ω and R_D=25Ω. These IF output powers decreased with increasing temperature but could be observed up to 75K.

These high frequency properties in the mm and sub-mm wave range clearly demonstrate the potential for high frequency applications using ramp-type JJs.

IV. Conclusions

We have successfully fabricated ramp-type JJs on MgO substrates using an STO buffer layer. The observed I_cR_n product for the JJs on STO buffered MgO was about 2mV at 4.2K and 0.1mV at 60K. The JJs clearly showed Shapiro steps up to 10mV under irradiation of mm-waves (100GHz) and 3rd Shapiro steps under irradiation of 0.762THz sub-mm-wave. Linewidth of Josephson emission at 50GHz from a JJ on a STO buffered MgO substrate was 4 times higher than the minimum possible one estimated by RSJ-model. We have also confirmed mixing in the self-oscillating mode using mm-wave and sub-mm-wave signals. These results showed that high-temperature superconducting ramp-type JJs on MgO substrates are promising for microwave applications, including the THz frequency band.

Acknowledgment

Josephson self-emission measurements were carried out by one of us at the Superconducting Electronics Laboratory, ISI, Research Center Jülich, Germany, using their experimental setup.

References

[1] M. A. J. Verhoeven, G. J. Gerristima, and H. Rogalla, "Ramp type HTS Josephson junctions with PrBaCuGaO barriers," *IEEE Trans. Appl. Supercond.*, vol. 5, pp. 2095–2098, 1995.

[2] H. Myoren, M. A. J. Verhoeven, J. Chen, K. Nakajima, T. Yamashita, D. H. A. Blank, and H. Rogalla, "High-Tc ramp-type Josephson junctions on MgO substrates for terahertz applications," *IEEE Trans. Appl. Supercond.*, vol. 8, pp. 132–136, 1998.

[3] M. A. J. Verhoeven, G. J. Gerristima, and H. Rogalla, "Ramp-type junctions with very thin PBCO barriers," *Proceeding of the Eucas '95 Conference*, Edinburgh, pp. 1395–1398, 1995.

[4] T. Minamikawa, T. Suzuki, Y. Yonezawa, K. Segawa, A. Morimoto, and T. Shimizu, "Annealing temperature dependence of MgO substrates on the quality of $YBa_2Cu_3O_x$ films prepared by pulsed laser ablation," *Jpn. J. Appl. Phys.*, Vol. 34, pp. 4038–4042, 1995.

[5] M. A. J. Verhoeven, G. J. Gerristima, and H. Rogalla, "Ramp-type junction parameter control by Ga doping of $PrBa_2Cu_3O_{7-\delta}$ barriers," *Appl. Phys. Lett.*, Vol. 69, pp. 848–850, 1996.

[6] K. K. Likharev, "Dynamics of Josephson junctions and circuits," Gordon and Breach Science Publishers, Paris, 1986.

[7] L. E. Amatuni, G. Kunkel, K. Y. Constantinian, L. Vonderbeck, K. Herrmann, M. Siegel and A. I. Braginski, "Spectral characteristics of the radiation emitted by a Josephson high-Tc YBCO step-edge junction," *Proceeding of the Eucas '95 Conference*, Edinburgh, pp. 1267–1270, 1995.

[8] L. E. Amatuni, L. Vonderbeck, A. M. Klushin and M. Siegel, "Josephson self-oscillator mixing experiments on step-edge junctions at millimeter wavelengths," *Proceeding of the Eucas '95 Conference*, Edinburgh, pp. 1685–1688, 1995.